VIP DNA Nanotechnology Very Important Paper

International Edition: DOI: 10.1002/anie.201710147
German Edition: DOI: 10.1002/ange.201710147

Folding DNA into a Lipid-Conjugated Nanobarrel for Controlled Reconstitution of Membrane Proteins

*Yuanchen Dong, Shuobing Chen, Shijian Zhang, Joseph Sodroski, Zhongqiang Yang, Dongsheng Liu, and Youdong Mao**

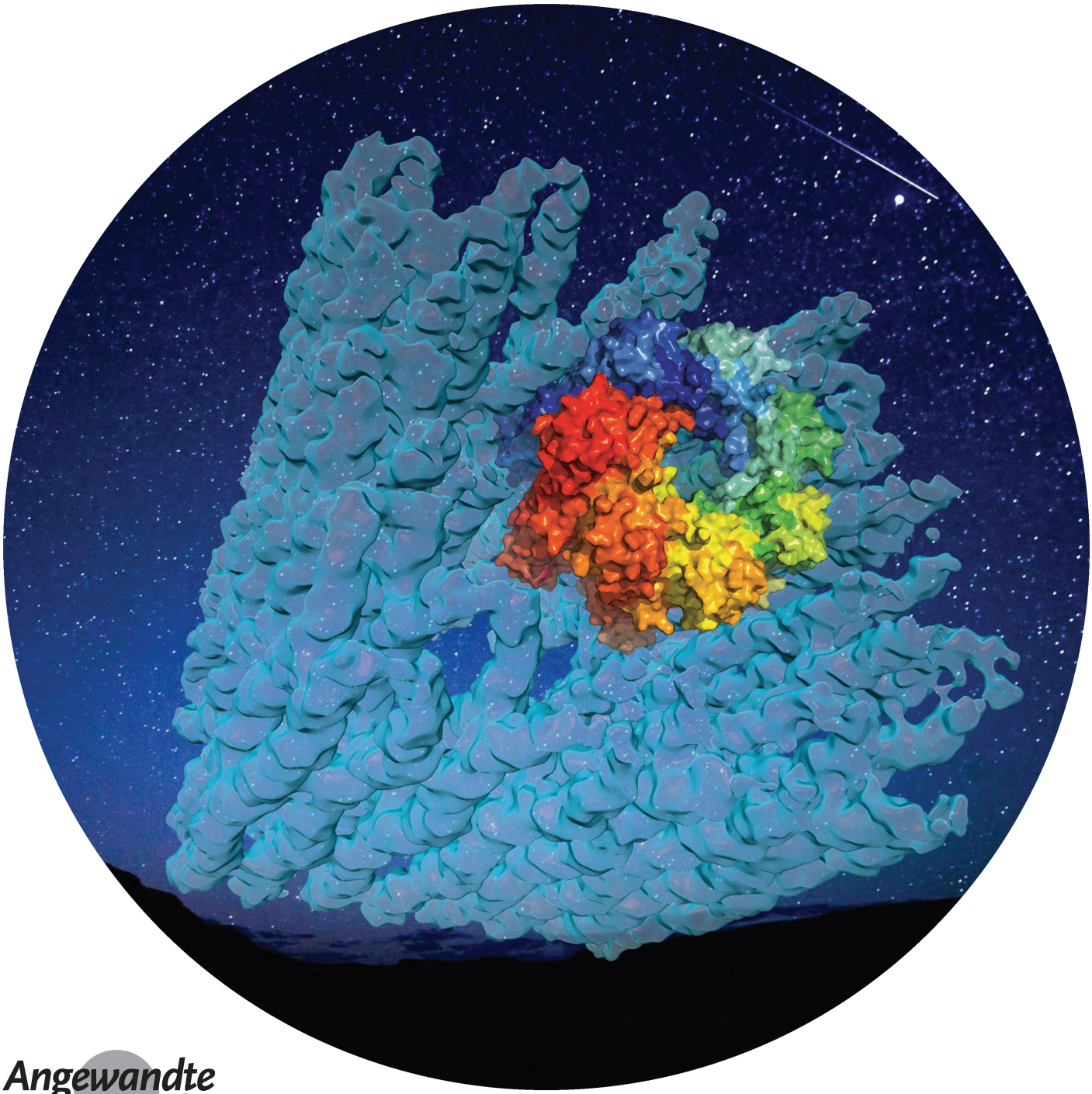

Abstract: *Building upon DNA origami technology, we introduce a method to reconstitute a single membrane protein into a self-assembled DNA nanobarrel that scaffolds a nanodisc-like lipid environment. Compared with the membrane-scaffolding-protein nanodisc technique, our approach gives rise to defined stoichiometry, controlled sizes, as well as enhanced stability and homogeneity in membrane protein reconstitution. We further demonstrate potential applications of the DNA nanobarrels in the structural analysis of membrane proteins.*

Membrane proteins are proteins integrated in the surface membrane of either cells or intracellular organelles. They play important roles in many fundamental biochemical processes, e.g., cellular signaling, ion transport, catalysis, metabolism, photosynthesis and cell adhesion.[1] Over 50% of all modern medicinal drugs were found to target membrane proteins.[1] Compared with soluble proteins, investigating the structures and functions of membrane proteins is generally challenging because it is difficult to maintain appropriate conformations of membrane proteins due to their reliance on the lipid bilayer environment and their poor stability and solubility upon removal from the cellular membrane.[2] Though several methods, including nanodiscs and liposome reconstitution, have been exploited to stabilize membrane proteins,[2,3] the utility of these systems for structural studies has been limited by the heterogeneity in sizes and the number of membrane proteins reconstituted to each nanodisc or liposome. During the last few decades, DNA nanotechnology has been well developed with its ability to form designed complex structures with precise control over nanoscale features in both static and dynamic ways.[4] DNA nanotechnology has also been successfully applied to manipulate molecules, nanoparticles and proteins, which demonstrated its potential applications in molecular and material sciences.[5] Here, taking advantage of the precisely programmable properties of DNA nanotechnology, we designed a DNA origami nanobarrel structure scaffolding a nanodisc-like lipid environment for controlled reconstitution of single membrane proteins.

Based on the principles of DNA origami construction,[6] a DNA nanobarrel was designed with the dimensions of approximately $20 \times 20 \times 30$ nm (Figure 1a, Figure S1 in the Supporting Information). An opening of $10 \times 10 \times 15$ nm and another opening of $5 \times 5 \times 15$ nm were introduced into the nanobarrel at the top and the bottom, respectively. Thus, an inner channel was expected to form as illustrated in Figure 1b. The detailed sequence design of staple strands and the annealing procedure are provided in Table S1 and Methods in the Supporting Information, respectively. Note that the channel size can be readily tuned for different sizes of membrane proteins through re-programming of DNA nanostructures.[6] Twelve single-stranded DNA (ssDNA) overhangs were left inside the DNA nanobarrel (Figure 1b), whose complementary strands were covalently conjugated to lipid molecules. The lipid molecules were anchored inside the nanobarrel through hybridization between the ssDNA overhangs and lipid-modified DNA (lipid-DNA) (Figure 1c). Prior to the hybridization, 2% octylglucoside (OG) detergent was introduced into the system to avoid detrimental aggregation of the lipid-DNA; then, the membrane protein was introduced to the system. The reconstitution was realized through a detergent removal procedure as illustrated in

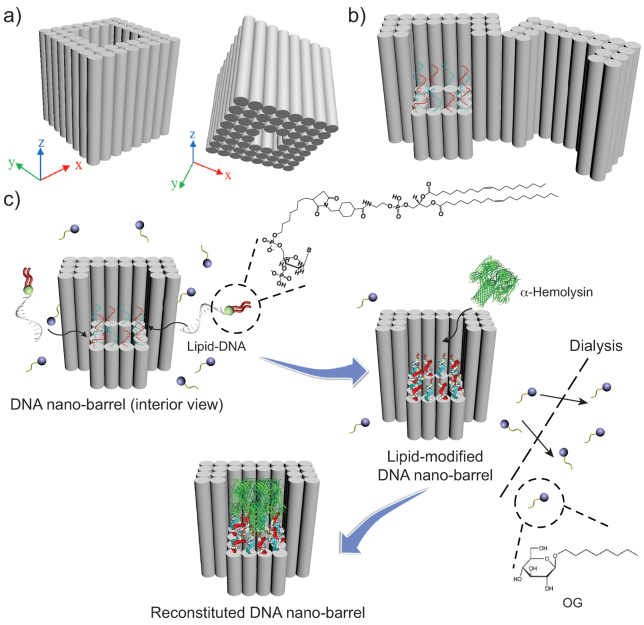

Figure 1. Reconstitution process: a) Different views of the design of the DNA nanobarrel with a central pore. The sequence design diagram is provided in Figure S1. Note that the exact end of the nanobarrel is not flat. Some short single strands were left at the end to avoid the aggregation of the DNA nanobarrel. These single-stranded spacers at the boundaries are not displayed in the schematic. b) The interior view of the DNA nanobarrel. Twelve ssDNA overhangs were introduced inside the nanobarrel for further hybridization with lipid-modified DNA. c) Reconstitution of α-hemolysin into the DNA nanobarrel through lipid–protein interaction following detergent removal. After the lipid molecules were anchored into the DNA nanobarrel, the α-hemolysin was incubated with the lipid-modified DNA nanobarrel. The reconstitution process was realized through dialysis against the buffer without the detergent.

[*] Dr. Y. Dong, Dr. S. Zhang, Dr. J. Sodroski, Dr. Y. Mao
Department of Cancer Immunology and Virology, Dana-Farber Cancer Institute, Department of Microbiology and Immunobiology, Harvard Medical School, Boston, MA 02115 (USA)
E-mail: youdong_mao@dfci.harvard.edu
Dr. Y. Dong, Dr. S. Chen, Dr. Y. Mao
Intel Parallel Computing Center for Structural Biology, Dana-Farber Cancer Institute, Boston, MA 02215 (USA)
Dr. S. Chen, Dr. Y. Mao
State Key Laboratory for Artificial Microstructures and Mesoscopic Physics, Institute of Condensed Matter and Material Physics, School of Physics, and Center for Quantitative Biology, Peking University Beijing 100871 (China)
Dr. Z. Yang, Dr. D. Liu
Key Laboratory of Organic Optoelectronics & Molecular Engineering of the Ministry of Education, Department of Chemistry, Tsinghua University, Beijing 100084 (China)
Supporting information and the ORCID identification number(s) for the author(s) of this article can be found under https://doi.org/10.1002/anie.201710147.

Figure 1c, in which the mixture of detergent-solubilized membrane protein, lipid-DNAs and DNA nanobarrels was dialyzed against a large reservoir of external buffer without the octylglucoside (OG) detergent.

After the annealing procedure, the self-assembled DNA nanobarrel was further purified by the polyethylene glycol (PEG) precipitation assay.[7] The formation of the DNA nanobarrel was confirmed by both agarose gel electrophoresis and transmission electron microscopy (TEM). In the agarose gel, a sharp band was observed after the annealing procedure, indicative of the formation of the nanobarrel assemblies (Figure S2). Using negative staining by uranyl formate, TEM images showed the designed cubic barrel geometry with a central channel (Figure 2a). Through single-particle image alignment and averaging,[8] the reference-free 2D class averages of over 1000 particles provided clear details of the DNA nanobarrel structure and the formation of the central channel (inset to Figure 2a, Figure S3). These results suggest that the DNA scaffold was self-assembled as expected.

To examine the feasibility of membrane protein reconstitution into the lipid-DNA nanobarrel, we chose a model protein α-hemolysin, which is a typical integral membrane protein well known for its important role in bacterial pathogenesis.[9] Seven monomers of α-hemolysin contribute to the formation of a barrel architecture with a 14-Å pore inside. The diameter of the outer domain of the α-hemolysin complex is ≈10 nm, which fits the dimensions of the designed lipid-DNA nanobarrel. After the reconstitution, due to selective molecular filtration through the dialysis membrane, OG molecules were diluted into the reservoir buffer and thus largely removed from the lipid-DNA/protein mixture, whereas both lipid-DNA nanobarrels and proteins were retained in the reconstitution system. Without the solubilizing effect of the OG detergent, the hydrophobic surface of the α-hemolysin transmembrane region should favor association with the hydrophobic tail of the lipid molecules in the DNA nanobarrel. Eventually, individual α-hemolysin complexes are expected to be captured by the DNA nanobarrel with a 1:1 stoichiometry. The reconstituted nanobarrels were further purified by glycerol gradient ultracentrifugation to remove the excess protein aggregates.[10]

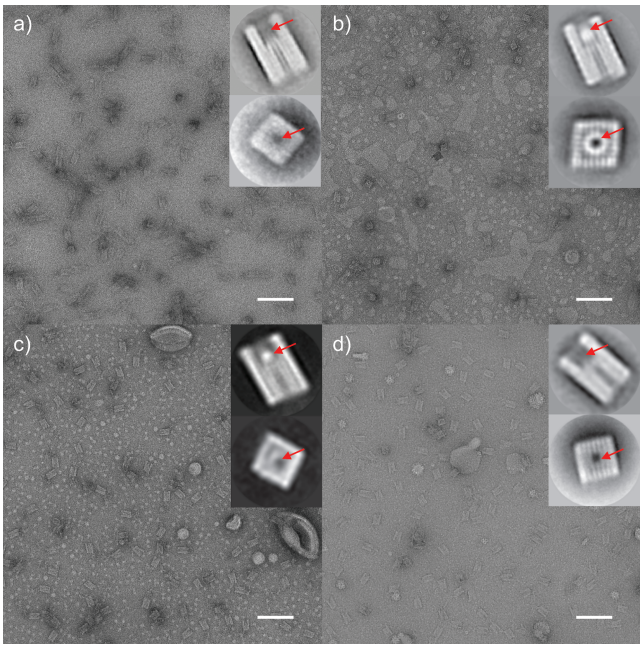

Figure 2. Negative-stain TEM analysis of the reconstitution process. a) TEM image of the designed DNA nanobarrel and a typical 2D class average image (right inset). As indicated by the arrow, the central channel was formed as designed. b) After α-hemolysin was reconstituted into the DNA nanobarrel as illustrated in Figure 1, the TEM image of the reconstituted DNA nanobarrel and its typical 2D class average image are displayed here. The feature of the protein was clearly observed as indicated by the arrow. c) The same experiment as in (b) was performed except that the α-hemolysin protein was not introduced. After the dialysis, the lipids inside the DNA nanobarrel aggregated into a micelle-like raft structure so that only a small spherical density can be observed in both the TEM image and its 2D class average. d) The DNA nanobarrels deprived of ssDNA-conjugated lipids were incubated with the α-hemolysin. After the same dialysis procedure, the protein was not reconstituted into the DNA nanobarrel as indicated by the arrow. In all panels, the scale bar is 50 nm. Dimension for the square of the 2D class averages is 39.1 nm.

To verify the reconstitution of α-hemolysin into the DNA nanobarrels, we used negative-stain TEM to visualize the supramolecular structures. In contrast to an empty channel in the DNA nanobarrel before the reconstitution procedure (Figure 2a), there was obvious additional density observed in the channel of the α-hemolysin-reconstituted DNA nanobarrels, as visualized in the corresponding 2D class averages of single-particle images (inset to Figure 2b and Figure S4). From the top view of the reconstituted nanobarrel, a spherical ring in the nanobarrel was observed, reminiscent of the homoheptameric β-barrel structure of α-hemolysin. The shape and size of this additional density closely match the structure of a single α-hemolysin complex, indicative of a successful reconstitution. No empty DNA nanobarrels were observed by 2D classification analysis on the negative-stain TEM images, suggesting a high efficiency of reconstitution. To further verify that the internal features arise from the reconstituted membrane protein but not the assembly of either detergents or lipid molecules, the detergent-removal experiment was repeated under the same conditions without α-hemolysin. In the resulting 2D class averages from negative-stain TEM, only a much smaller density was seen inside the nanobarrel (Figure 2c, Figure S5). This density lacked the features of α-hemolysin, and may be attributed to the formation of a nanoscale lipid assembly anchored inside the DNA nanobarrel via the ssDNA-conjugated lipids. In another control experiment, the DNA nanobarrels deprived of ssDNA-conjugated lipids were incubated with the α-hemolysin. As expected, these lipid-deprived DNA nanobarrels appeared empty, without the density associated with α-hemolysin (Figure 2d, Figure S6). These results indicate that the ssDNA-conjugated lipid molecules are responsible for the success of membrane protein reconstitution.

To demonstrate the versatility of our strategy, another integral membrane protein, trimeric envelope glycoprotein (Env) from the human immunodeficiency virus type 1 (HIV-1),[11] was also reconstituted into the DNA nanobarrels through a detergent removal procedure (Figure S7). After the reconstitution, similar results were obtained (Figure S8

and S9). There was obvious additional density inside the DNA nanobarrel corresponding to the Env proteins as compared with the empty DNA nanobarrels. This result supports that our reconstitution strategy is not specific to a given membrane protein, and should be generally applicable to other membrane proteins whose sizes are compatible with designed lipid-conjugated DNA nanobarrels.

To demonstrate the potential applications in structural investigation of membrane proteins by our reconstitution method, we further employed cryo-EM and single-particle analysis to characterize the 3D structure of α-hemolysin through the reconstituted nanobarrel. Due to the low contrast of cryo-EM for such a small protein compared with DNA nanobarrel, the α-hemolysin was not as clear in raw single-particle images as those in the negative-stain TEM images (Figure 3a). However, in the 2D class averages, the features of α-hemolysin became obvious (Figure 3b). Single-particle reconstruction and cryo-EM refinement yielded a 3D density map of the α-hemolysin-reconstituted DNA nanobarrel (Figure 3c and d). The overall resolution of the density map was measured to be around 7.5 Å through a gold-standard Fourier shell correlation (FSC).[12] The local resolution calculated by the ResMap program suggests that the central part of the DNA nanostructure achieves a resolution of around 6–8 Å, whereas the surface elements are in the 8–9 Å resolution range[13] (Figure 3c and Figure S10). The density quality is sufficient to allow reasonable backbone fitting of the DNA (Figure 3d and e).

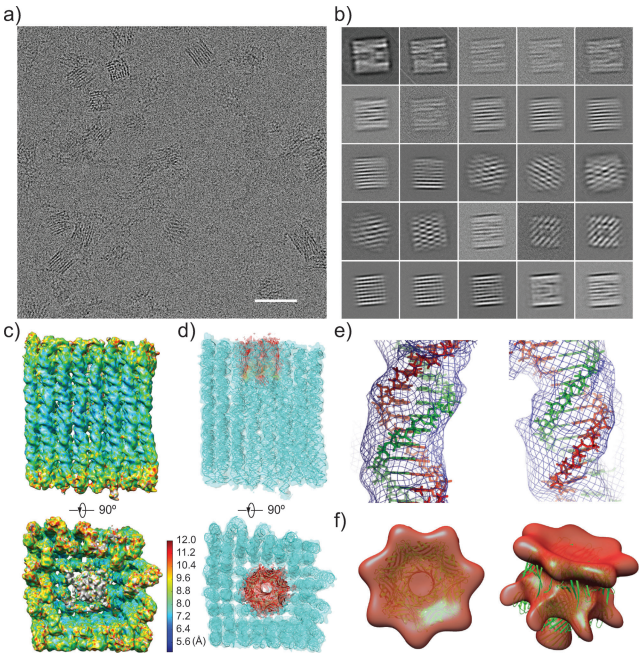

Figure 3. Cryo-EM visualization of the reconstituted DNA nanobarrel. a) A typical cryo-EM micrograph of reconstituted DNA nanobarrel with α-hemolysin. Scale bar is 50 nm. b) A gallery of typical reference-free 2D class averages of the α-hemolysin-reconstituted nanobarrel computed by the ROME software.[14] c) The cryo-EM density map of the α-hemolysin-reconstituted DNA nanobarrel is shown in two orthogonal views, and is colored according to the local resolution. d) The pseudo-atomic model in a ribbon representation fitted with the cryo-EM density map, shown in two orthogonal views that are the same as those shown in (c). The DNA and protein components are colored cyan and red, respectively. e) Representative cryo-EM density superimposed with the atomic model of a DNA double helix in stick representation. The cryo-EM density allows good fitting of the DNA double helix backbone. The bumpy shape of the sugar ring or phosphate group can also be recognized. f) The cryo-EM density map of the α-hemolysin after the refinement using the density-subtracted single-particle images, viewed from two orientations. The atomic model from the crystal structure of α-hemolysin was fitted into the map.

Compared with the DNA part, the resolution of the α-hemolysin is much lower, with the consequence that no high-resolution features can be discerned in the density map (Figure 3c and d). This might well result from the inevitable rotational and vibrational movement of the α-hemolysin protein relative to the DNA nanobarrel scaffold, because there is no physical constraint on the in-plane rotational orientations of the α-hemolysin against the DNA nanobarrel (Figure S11). To counteract these dynamic effects, we subtracted the density of DNA nanobarrel from the raw single-particle images. Using the DNA-density-subtracted images, the density map of α-hemolysin was reconstructed and refined with imposing *C*7 symmetry at a resolution of around 30 Å. As illustrated in Figure 3f, the features of the outer and transmembrane domains of α-hemolysin become apparent. The atomic model of the α-hemolysin can be readily fitted into the density map as a rigid body. Although the current resolution is not very high partly due to a sub-optimal procedure of density subtraction, the result suggests potential applications of our method in the biophysical analysis of membrane proteins with further improvement on both cryo-EM and DNA nanotechnology.

In summary, we have proved the general principle of a novel method to reconstitute individual membrane proteins into lipid-conjugated DNA nanobarrel structures in vitro. By careful design, both single α-hemolysin and HIV-1 Env trimer proteins have been incorporated into a DNA nanobarrel in a monodispersed and native-like state. We further demonstrated the potential of our approach in investigating membrane protein structures. The key advantage of this approach over the membrane-scaffolding-protein nanodisc technique[2,3] lies in a higher degree of programmability of DNA origami nanostructures,[6] which potentially allows permutations in the design of the DNA nanobarrel to match a great diversity of membrane proteins of different sizes. However, potential difficulties may exist for the reconstitution of multi-subunit membrane protein complexes like HIV-1 Env, owing to their intrinsic metastability and their labile interactions with detergents and lipids. Additional strategic modifications, such as introducing ligand anchors or choices of specific detergent or lipid molecules might mitigate these problems via stabilization of the entire reconstituted superstructures. In combination with DNA modification and dynamic assembly of DNA nanostructures,[4a,c–e,5] our approach provides a powerful way to create hybrid supramolecular systems from three types of molecules essential for life—DNA, protein and lipid, the inclusion of which may be crucial for the development of potential applications in nanomedicine and nanorobotics.

Acknowledgements

This work was funded in part by an Intel academic grant (Y.M.), by a grant of the Thousand Talents Plan of China (Y.M.), by grants from National Natural Science Foundation of China No. 11774012, 91530321 (Y.M.) and 91427302 (D.L.), and by grants from the National Institutes of Health (NIH) of the United States AI93256, AI24982, AI100645 and AI24755 (J.S.). The cryo-EM experiments were performed in part at the Center for Nanoscale Systems at Harvard University, a member of the National Nanotechnology Coordinated Infrastructure Network (NNCI), which is supported by the National Science Foundation under NSF award no. 1541959. The cryo-EM facility was funded through the NIH grant AI100645, Center for HIV/AIDS Vaccine Immunology and Immunogen Design (CHAVI-ID). The data processing was performed in part in the Sullivan cluster, which is funded in part by a gift from Mr. and Mrs. Daniel J. Sullivan, Jr. The accession numbers for the cryo-EM map and pseudo-atomic model of the DNA nanobarrel are Electron Microscopy Data Bank EMD-7304 and PDB ID 6BY7.

Conflict of interest

The authors declare no conflict of interest.

Keywords: cryo-EM · DNA nanotechnology · DNA origami · membrane protein reconstitution · single-particle analysis

How to cite: *Angew. Chem. Int. Ed.* **2018**, *57*, 2072–2076
Angew. Chem. **2018**, *130*, 2094–2098

[1] D. Whitford, *Proteins: Structure and Function*, Wiley, Hoboken, **2005**.
[2] N. Vaidehi, J. Klein-Seetharaman, *Membrane Protein Structure and Dynamics: Methods and Protocols*, Humana Press, New York, **2012**.
[3] a) T. H. Bayburt, Y. V. Grinkova, S. G. Sligar, *Nano Lett.* **2002**, *2*, 853–856; b) J. Frauenfeld, J. Gumbart, E. O. Sluis, S. Funes, M. Gartmann, B. Beatrix, T. Mielke, O. Berninghausen, T. Becker, K. Schulten, R. Beckmann, *Nat. Struct. Mol. Biol.* **2011**, *18*, 614–621; c) C. Yoshiura, Y. Kofuku, T. Ueda, Y. Mase, M. Yokogawa, M. Osawa, Y. Terashima, K. Matsushima, I. Shimada, *J. Am. Chem. Soc.* **2010**, *132*, 6768–6777.
[4] a) N. C. Seeman, *Annu. Rev. Biochem.* **2010**, *79*, 65–87; b) M. R. Jones, N. C. Seeman, C. A. Mirkin, *Science* **2015**, *347*, 1260901; c) S. M. Douglas, H. Dietz, T. Liedl, B. Högberg, F. Graf, W. M. Shih, *Nature* **2009**, *459*, 414–418; d) P. W. Rothemund, *Nature* **2006**, *440*, 297–302; e) M. M. Shih, J. D. Quispe, G. F. Joyce, *Nature* **2004**, *427*, 618–621.
[5] a) D. S. Liu, E. J. Cheng, Z. Q. Yang, *NPG Asia Mater.* **2011**, *3*, 109–114; b) X. Quyang, M. De Stefano, A. Krissanaprasit, A. L. B. Kodal, C. B. Rosen, T. Liu, S. W. Helmig, C. Fan, K. V. Gothelf, *Angew. Chem. Int. Ed.* **2017**, *56*, 14423–14427; *Angew. Chem.* **2017**, *129*, 14615–14619.
[6] Y. Ke, S. M. Douglas, M. Liu, J. Sharma, A. Cheng, A. Leung, Y. Liu, W. M. Shih, H. Yan, *J. Am. Chem. Soc.* **2009**, *131*, 15903–15908.
[7] E. Stahl, T. G. Martin, F. Praetorius, H. Dietz, *Angew. Chem. Int. Ed.* **2014**, *53*, 12735–12740; *Angew. Chem.* **2014**, *126*, 12949–12954.
[8] S. H. Scheres, *J. Struct. Biol.* **2012**, *180*, 519–530.
[9] a) T. Sugawara, D. Yamashita, K. Kato, Z. Peng, J. Ueda, J. Kaneko, Y. Kamio, Y. Tanaka, M. Yao, *Toxicon* **2015**, *108*, 226–231; b) O. V. Kovalevskiy, A. A. Lebedev, A. K. Surin, A. S. Solonin, A. A. Antson, *J. Mol. Biol.* **2007**, *365*, 825–834.
[10] C. Lin, S. D. Perrault, M. Kwak, F. Graf, W. M. Shih, *Nucleic Acids Res.* **2013**, *41*, e40.
[11] Y. Mao, L. Wang, C. Gu, A. Herschhorn, S. H. Xiang, H. Haim, X. Yang, J. Sodroski, *Nat. Struct. Mol. Biol.* **2012**, *19*, 893–899.
[12] S. H. Scheres, S. Chen, *Nat. Methods* **2012**, *9*, 853–854.
[13] A. Kucukelbir, F. J. Sigworth, H. D. Tagare, *Nat. Methods* **2014**, *11*, 63–65.
[14] J. Wu, Y. B. Ma, C. Congdon, B. Brett, S. Chen, Q. Ouyang, Y. Mao, *PLoS One* **2017**, *12*, e0182130.

Manuscript received: October 1, 2017
Revised manuscript received: December 6, 2017
Accepted manuscript online: December 20, 2017
Version of record online: January 9, 2018

